Neuropharmacology 265 (2025) 110242

Contents lists available at ScienceDirect

Neuropharmacology

journal homepage: www.elsevier.com/locate/neuropharm

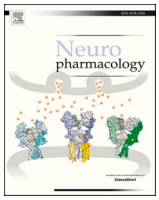

GPR88 impairs the signaling of kappa opioid receptors in a heterologous system and in primary striatal neurons

Rafael Rivas-Santisteban [a,b,**], Jaume Lillo [b,c], Claudia Garrigós [c], Gemma Navarro [b,e], Rafael Franco [b,c,d,*]

[a] Laboratory of Computational Medicine, Biostatistics Unit, Faculty of Medicine, Autonomous University of Barcelona, Campus Bellaterra, 08193, Barcelona, Spain
[b] Network Center for Biomedical Research in Neurodegenerative Diseases. CiberNed., Spanish National Health Institute Carlos iii, Av. Monforte de Lemos, 3-5, 28029, Madrid, Spain
[c] Molecular Neurobiology Laboratory, Dept. Biochemistry and Molecular Biomedicine, Facultat de Biologia, Universitat de Barcelona, 08028, Barcelona, Spain
[d] School of Chemistry, Universitat de Barcelona, Barcelona, Spain
[e] Department of Biochemistry and Physiology, School of Pharmacy and Food Sciences, Universitat de Barcelona, 08028, Barcelona, Spain

ARTICLE INFO

Handling Editor: T. Di Paolo

Keywords:
Parkinson's disease
Striatopallidal neurons
Striatonigral neurons
cAMP
Mitogen-activated protein kinase MAPK
Kappa opioid receptor
Direct pathway
Basal ganglia
Reward circuit
Pain

ABSTRACT

The physiological role of GPR88, an orphan G protein-coupled receptor (GPCR) predominantly expressed in the striatum, remains unclear, despite its altered expression in parkinsonian animal models. GPR88 is known to interact with other GPCRs. Specifically, GPR88 expression inhibits signaling mediated by the μ-opioid receptor in cells coexpressing both receptors. The effect of GPR88 on the kappa-opioid receptor (KOR) is less understood. In this study, we examine the interaction between GPR88 and KOR, and the impact of GPR88 expression on KOR-mediated signaling in heterologous cells and primary striatal neurons. Bioluminescence resonance energy transfer and proximity ligation assays revealed an interaction between GPR88 and KOR. Functional assays showed that GPR88 antagonized the effects of U69,593, a selective KOR agonist, on forskolin-stimulated cAMP levels, β-arrestin-2 recruitment, and phosphorylation of extracellular signal-regulated kinases (ERK1/2) in HEK-293T cells coexpressing both receptors. In primary striatal neurons, GPR88 and KOR complexes were observed, with KOR activation effects enhanced when GPR88 expression was suppressed using RNA interference. These results suggest that GPR88 and KOR are coexpressed in striatal neurons, where GPR88 inhibits KOR activation. Notably, the GPR88-KOR heteromer was more prevalent in dopamine D_1-receptor-containing neurons of the direct pathway of the basal ganglia. Given the roles of KORs in dopamine release, motor function regulation, and pain and reward perception, the GPR88-KOR interaction warrants further investigation in the context of neuropathic pain, Parkinson's disease, and neuropsychiatric disorders.

1. Introduction

GPR88 is an orphan G protein-coupled receptor (GPCR) previously known as striatum-specific GPCR (Mizushima et al., 2000; Alexander et al., 2023). Despite its expression in medium spiny neurons and neurons of the thalamus, the olfactory tubercle and the cortex, its endogenous agonist is unknown and its function remains undeciphered (Waes et al., 2011; Massart et al., 2009). However, a relevant role of the receptor is suspected due to the association of a mutation in the GPR88 gene with a familial disease known as COCPMR (Chorea, Childhood-Onset, with Psychomotor Retardation) (Alkufri et al., 2016). Expression regulation by glutamatergic and dopaminergic afferents and unbalanced expression in the striatal output pathways in a rodent model of Parkinson's disease led to the proposal of GPR88 as a therapeutic target of the disease (Massart et al., 2009). In the absence of the receptor, GABAergic medium spiny neurons (MSNs) reduce their inhibitory potential, leading to an increased glutamatergic tone (Quintana et al., 2012). Gpr88 knockout mice show altered dopaminergic neurotransmission and increased sensitivity to amphetamine-stimulated locomotor activity and apomorphine-induced motor and stereotypic cues

* Corresponding author. Department of Biochemistry and Molecular Biomedicine, Faculty of Biology, Universitat de Barcelona, 08028, Barcelona, Spain.
** Corresponding author. Laboratory of Computational Medicine, Biostatistics Unit, Faculty of Medicine, Autonomous University of Barcelona, Campus Bellaterra, 08193, Barcelona, Spain.
E-mail addresses: rrivasbioq@gmail.com (R. Rivas-Santisteban), rfranco@ub.edu, rfranco123@gmail.com (R. Franco).

https://doi.org/10.1016/j.neuropharm.2024.110242
Received 20 June 2024; Received in revised form 14 November 2024; Accepted 26 November 2024
Available online 28 November 2024
0028-3908/© 2024 The Authors. Published by Elsevier Ltd. This is an open access article under the CC BY-NC license (http://creativecommons.org/licenses/by-nc/4.0/).

(Logue et al., 2009). On waiting for the discovery of the endogenous ligand, significant evidence shows that GPR88 may interact with various GPCRs, thus appearing as a potential modulator of their expression and/or signaling. Laboute et al., 2020, showed that GPR88 may form heteromers with some types of opioid, adenosine, dopamine, muscarinic and chemokine receptors (Laboute et al., 2020).

Opioid receptors consist of four types of GPCRs activated by endogenous peptides and by natural and synthetic opioids. Mu opioid receptors are activated by endorphins, delta receptors by enkephalins, kappa receptors (KORs) by dynorphins, and nociceptin (ORL-1 or NOP) receptors by nociceptin (Alexander et al., 2023). Opioid receptors can inhibit the transmission of pain signals within the central nervous system (CNS), effectively reducing the sensation of pain. These receptors are also involved in the brain's reward systems. Activation of opioid receptors in certain brain regions (such as the ventral tegmental area and nucleus accumbens) leads to feelings of pleasure and euphoria (Wang, 2019).

Tyr-D-Ala-Gly-N-MePhe-Gly-ol (DAMGO), an agonist of the μ-opioid receptor, inhibits forskolin-induced cAMP production and activates the mitogen-activated protein kinase (MAPK) signaling pathway. Studies in heterologous systems have demonstrated that coexpression of GPR88 and μ-opioid receptors reduces DAMGO's effects on both cAMP levels and ERK phosphorylation. Additionally, GPR88 expression decreases the affinity of β-arrestin-2 for the activated μ-opioid receptor. Notably, GPR88 is enriched in the striatum, where kappa opioid receptors (KORs) play critical roles in modulating motor function, reward pathways, and GABAergic transmission (Trifilieff and Martinez, 2013).

In the striatum, KORs are expressed in MSNs as well as on GABAergic interneurons, and they are implicated in the modulation of synaptic transmission and behavioral responses to reward and stress (Brooks and O'Donnell, 2017). Evidence suggests that KORs are present in specific striatal circuits, including direct and indirect MSNs, where they interact with multiple neuromodulatory systems (Escobar, 2017). This overlap with GPR88, which is predominantly localized in MSNs, suggests potential interactions between KORs and GPR88 that could influence striatal signaling dynamics and behavior. Given this anatomical and functional alignment, the present study aimed to investigate whether GPR88 expression modulates KOR functionality within the striatum, thereby contributing to the region's regulation of motor and reward-related processes.

2. Methods

2.1. Reagents

Forskolin (FK, ref. F3917), U69,593 (ref. U103-5 MG), Poly-EthylenImine (PEI, ref. 408727) and Hoechst 33432 (ref. 14533) were purchased from Sigma-Aldrich (St Louis, MO, USA) and JDTic, a KOR antagonist, from MedChemExpress (Cat. No.: HY-10487). Concentrated (10 mM) stock solutions prepared in dimethyl sulfoxide were stored at −20 °C; they were thawed and diluted before use.

2.2. Cell culture

HEK-293T cells, batch 70022180, were acquired from the American Type Culture Collection (ATCC). Cells were amplified and frozen in liquid nitrogen in several aliquots. Cells from each aliquot were used until passage 18. HEK-293T cells were grown in Dulbecco's modified Eagle's medium (DMEM) (ref. D5796-500 ML, Gibco, Paisley, Scotland, UK) supplemented with 2 mM L-glutamine, 100 μg/mL sodium pyruvate, 100 U/mL penicillin/streptomycin, MEM non-essential amino acids solution (1/100) and 5% (v/v) heat-inactivated fetal bovine serum (FBS) (all supplements were from Invitrogen, Paisley, Scotland, UK) and maintained at 37 °C in a humid atmosphere of 5% CO_2.

Primary striatal neurons were obtained from 19-day mouse embryos as elsewhere described (Hradsky et al., 2013; Franco et al., 2018). Briefly, striata were dissected and digested in 0.25% trypsin (Gibco, ref. 12605-028) for 15 min at 37 °C. Trypsinization was stopped by repeated washes with Hank's Buffered Saline Solution (HBSS, Gibco). Cells were brought to a single-cell suspension by repeated pipetting followed by passage through a 100 μm-pore mesh. Cells were then resuspended in supplemented DMEM and seeded at a density of 3.5×10^5 cells/mL in six-well (Cultek, ref. 3506) or 96-well plates (Cultek, ref. 3596) for functional assays and in twelve-well plates (Cultek, ref. 3512) for immunocytochemistry or PLA. 24 h later the medium was replaced by neurobasal medium supplemented with 2 mM L-glutamine, 100 U/mL penicillin/streptomycin, and 2% (v/v) B27 (Gibco, ref. 17504044) and cells were cultured for 12 days. Cultures were maintained at 37 °C in a 5% CO_2 humid atmosphere. Immunodetection of the NeuN-Alexa488 antibody marker (Abcam, ref. EPR12763) showed that preparations contained >95% neuronal cells.

2.3. Cell transfection

HEK-293T cells were transiently transfected with the corresponding cDNA(s) using PolyEthylenImine (PEI). Briefly, cDNA diluted in 150 mM NaCl was mixed (10 min) with PEI (5.5 mM in nitrogen residues). The cDNA-PEI complexes were placed in contact with HEK-293T cells and were incubated for 4 h in a serum-free medium. Then, the medium was replaced by a fresh supplemented culture medium and cells were maintained at 37 °C in a 5% CO_2 humid atmosphere. 48 h after transfection, cells were washed, detached, and resuspended in the assay buffer.

2.4. Expression vectors

pcDNA3.1-based plasmids encoding for GPR88 (human version), KOR (human version) GPR88-Rluc, KOR-YFP and ghrelin receptor-YFP were used. Plasmids encoding fusion proteins (GPR88-Rluc, KOR-YFP and ghrelin receptor-YFP) were generated by subcloning the coding region of each receptor to be in-frame with restriction sites of pRluc-N1 (Clontech, Heidelberg, Germany) and pEYFP-N1 (PerkinElmer, Waltham, MA, US) vectors to provide plasmids that express the receptors with Rluc or YFP proteins fused on the C-terminal end.

2.5. Bioluminescence resonance energy transfer (BRET) assay

HEK-293T cells were transiently cotransfected with a constant amount of cDNA encoding for GPR88-Rluc (0.2 μg) and with increasing amounts of cDNA corresponding to either KOR-YFP (0.5–4.5 μg), or with ghrelin receptor-YFP (0.25–2 μg), as a negative control for BRET assay. To assess cell amount, protein concentration was determined using a Bradford assay kit (Bio-Rad, Munich, Germany) using bovine serum albumin dilutions as standards, and the amount of cells was adjusted to 20 μg of protein using a Bradford assay kit (Bio-Rad, Munich, Germany). To quantify protein-YFP expression, fluorescence was read in a Mithras LB 940 equipped with a high-energy xenon flash lamp, using a bandwidth excitation filter at 395 nm. For BRET measurements, the equivalent to 20 μg protein cell suspension was distributed in 96-well microplates (white plates, ref. 11457009) Porvair, Leatherhead, UK) and coelenterazine (5 μM) was added (PJK GMBH, Kleinblittersdorf, Germany). 30 s after coelenterazine addition, the readings were collected using a Mithras LB 940 reader (Berthold Technologies, DLReady, Germany), which allows the integration of the signals detected in the short-wavelength filter at 485 nm and the long-wavelength filter at 530 nm. To quantify receptor-Rluc expression, luminescence readings were collected 10 min after adding coelenterazine (5 μM) (Molecular Probes, Eugene, OR) using a Mithras LB 940. MilliBRET units (mBU) are defined as:

$$\mathrm{mBU} = \left[\frac{\lambda_{530}(\mathrm{long-wavelength\ emission})}{\lambda_{485}(\mathrm{short-wavelength\ emission})} - C_f \right] x\,1000$$

where C_F, corresponds to [(long-wavelength emission)/short-wavelength emission)] for cells only expressing the Rluc-containing donor. Therefore, $BRET_{MAX}$ is defined as the maximal achievable value of BRET, and this circumstance occurs when all available donor receptors are paired up with acceptor receptors. Accordingly, $BRET_{50}$ is defined as the acceptor/donor ratio at which 50% of the $BRET_{MAX}$ is achieved.

2.6. cAMP determination

Determination of intracellular 3′,5′-monophosphate (cAMP) levels was performed in primary neurons or HEK-293T cells transfected with the cDNA for GPR88 (1.5 μg), the cDNA for the KOR (1.5 μg) or both. The intracellular concentration of this first messenger was determined using the Lance Ultra cAMP kit (PerkinElmer). The method consists of a time-resolved fluorescence resonance energy transfer (TR-FRET) immunoassay in which endogenous cAMP competes with europium (Eu) chelate-labeled cAMP tracer for binding sites on a cAMP-specific antibody labeled with the ULight™ dye. Light pulses at 320 nm excite the Eu of the tracer. The energy emitted by the excited Eu to is transferred to ULight molecules on the antibodies, which in turn emit light at 665 nm. In the absence of cAMP, maximal TR-FRET signal is achieved; when an agonist leads to an increase in cytosolic cAMP levels the competition between the unlabeled and the Eu-labeled cAMP species leads to a decrease in the TR-FRET signal, the emission fluorescence remains unmodified when equilibrium is achieved. cAMP concentrations per cell or mg protein were determined using a standard curve using unlabeled cAMP. Residual energy from the Eu chelate will produce light at 615 nm. The dynamic range is 10^{-10} to 10^{-8} M.

Neurons or transfected cells were grown in 6-well plates. 48 h post-transfection, the medium was replaced by serum-free medium (DMEM). Two hours later cells were detached, isolated by centrifugation (5 min at 1500 rpm) and resuspended in ^{cAMP}medium, which consisted of DMEM containing HEPES (5 mM, pH 7.4), zardaverine (50 μM), a phosphodiesterase inhibitor to prevent degradation of cAMP, and 0.1% bovine serum albumin (BSA, Merck, ref. D5796). Determination was performed in 384-well plates (PerkinElmer) using 4000 cells/well.

Cells were incubated for 15 min with 2 μl of ^{cAMP}medium (to determine the basal levels of cAMP) or with 2 μl of the KOR agonist prepared in ^{cAMP}medium. 15 min after agonist addition, cells were treated for 15 min with 500 nM forskolin (FK). cAMP-Europium (cAMP-Eu) (5 μl) and fluorophore-containing ULight™ antibody (5 μl) were then added. Incubation was prolonged for 1 h at 25 °C and the PHERAstar Flagship reader equipped with an HTRF optical module (BMG Lab Technologies, Offenburg, Germany) was used for measuring the 665/620 nm ratio.

2.7. ERK1/2 phosphorylation assay

The assay was performed in transfected HEK-293T cells (48 h post-transfection with cDNAs for GPR88 -1 μg- and/or KOR -1 μg-). Two hours before initiating the experiment, the culture medium was replaced by a serum-free DMEM medium. Cells were incubated at 37 °C with U69,593, a selective KOR agonist. After 7 min the reaction was stopped by placing cells on ice. Then, cells were washed twice with cold Phosphate Buffered Saline (PBS) and lysed by the addition of ice-cold lysis buffer (50 mM Tris-HCl pH 7.4, 50 mM NaF, 150 mM NaCl, 45 mM ß-glycerol-phosphate, 1% Triton X-100, 20 μM phenyl-arsine oxide, 0.4 mM $NaVO_4$ and protease inhibitor mixture (Sigma-Aldrich, St. Louis, MO, USA). Cellular debris were removed by centrifugation at 13,000 g for 10 min at 4 °C, and protein concentration was adjusted to 1 mg/mL by the bicinchoninic acid method (ThermoFisher Scientific, Waltham, MA, USA) using a commercial BSA dilution (ThermoFisher Scientific) for standardization. 6x Laemli SDS sample buffer (300 mM Tris-Base, 600 mM DTT, 40% glycerol (v/v), 0.012 % bromophenol blue (w/v) and 12 % SDS (w/v), pH = 6,8) was added to the samples and proteins were denatured by boiling at 100 °C for 5 min. ERK1/2 phosphorylation was determined by Western blot. Equivalent amounts of protein (20 μg) were subjected to electrophoresis (10% SDS-polyacrylamide gel) and transferred onto PVDF membranes (Immobilon-FL PVDF membrane, MERCK, St. Louis, MO, USA) for 30 min using Trans-Blot Turbo system (Bio-Rad). Then, the membranes were blocked for 2 h at room temperature (constant shaking) with Odyssey Blocking Buffer (LI-COR Biosciences, Lincoln, NE, USA) and labeled with a mix of primary mouse anti-phospho-ERK1/2 (1:2500, MERCK, Ref. M8159) and rabbit anti-ERK1/2 (1:40,000, MERCK, Ref. M5670) antibodies overnight at 4 °C with shaking. Then, the membranes were washed three times with PBS containing 0.05% tween for 10 min and subsequently were incubated with a mix of IRDye 800 anti-mouse (1:10,000, MERCK, Ref. 92632210) and IRDye 680 anti-rabbit (1:10,000, MERCK, Ref. 926–68071) secondary antibodies for 2 h at room temperature, light-protected. Membranes were washed 3 times with PBS-tween 0.05% for 10 min and once with PBS and left to dry. Bands were analyzed using Odyssey infrared scanner (LI-COR Biosciences). Band densities were quantified using Fiji software, and the level of phosphorylated ERK1/2 was normalized using the intensities of the total ERK1/2 protein bands. The effect of the KOR agonist, U69,593, was given in percentage respect to the reference value (basal). The value achieved without the agonist, i.e. adding 30 μl DMEM, was taken as a reference (normalizing the basal to 100%).

For striatal neurons, cells were plated in transparent Deltalab 96-well microplates and after 10 DIV were transfected with the transfection protocol detailed in section 2.10 (below). Two hours before initiating the experiment, the culture medium was replaced by serum-free DMEM medium. Then, cells were treated or not for 10 min with the selective antagonist for KOR (JDTic (1 μM) followed by 7 min treatment with the selective agonist for KOR (U69,593 1 nM-10 μM). Cells were then washed twice with cold PBS before the addition of lysis buffer (15 min treatment). Ten microliters of each supernatant were placed in white ProxiPlate 384-well microplates and ERK1/2 phosphorylation was determined using an AlphaScreen®SureFire® kit (PerkinElmer) following the instructions of the supplier and using an EnSpire® Multimode Plate Reader (PerkinElmer).

2.8. β-arrestin-2 recruitment assay

HEK-293T cells were transiently cotransfected with cDNA coding for ß-arrestin-2-Rluc and with cDNA coding for KOR-YFP. BRET experiments were performed 48 h after transfection. Cells were detached using HBSS containing 0.1% glucose, centrifuged for 5 min at 3200 rpm and resuspended in the same buffer. Protein concentration was quantified by using the Bradford assay kit (Bio-Rad, Munich, Germany) and adjusted to 0.2 mg/mL. Hereafter, YFP fluorescence was quantified at 530 nm in a FluoStar Optima Fluorimeter (BMG Labtech, Offenburg, Germany) to quantify receptor-YFP expression upon excitation at 488 nm. To measure β-arrestin-2 recruitment, cells (20 μg of protein) were distributed in 96-well microplates (Corning 3600, white plates with white bottom). Cells were then stimulated with U69,593 before the addition of 5 μM coelenterazine H (Molecular Probes, Eugene, OR). BRET between β-arrestin 2-Rluc and receptor-YFP was determined and quantified 1 min after adding coelenterazine H. The readings were collected using a Mithras LB 940 (Berthold Technologies, Bad Wildbad, Germany), which allows the integration of the signals detected in the short-wavelength filter (485 nm) and the long-wavelength filter (530 nm). To quantify protein-Rluc expression, luminescence readings were also collected 10 min after the addition of 5 μM coelenterazine H.

2.9. Immunocytochemistry

Cells were fixed in 4% paraformaldehyde for 15 min and washed twice with PBS containing 20 mM glycine before permeabilization with PBS-glycine containing 0.2% Triton X-100 (10 min incubation). Then, cells were incubated with a mouse monoclonal anti-Rluc primary

antibody (1/100, MAB4400, Millipore, Merck, Darmstadt, Germany) for 1 h and subsequently were washed and incubated with a secondary Cy3-conjugated anti-mouse IgG antibody (1/200; Jackson ImmunoResearch, West Grove, PA, USA) (red).

In all cases, nuclei were stained with Hoechst 33432 (1/100 from 1 mg/mL stock; Sigma-Aldrich). Samples were washed several times and stored in Immu-mount® (ThermoFisher). Images were obtained in a Zeiss LSM 880 confocal microscope (Zeiss, Jena, Germany) with a 63x oil objective.

2.10. *In situ* proximity ligation assay

The *in situ* proximity ligation assay (PLA) allows identifying protein protein interactions. The interaction between GPR88 and KOR in striatal neurons and brain sections was detected using the Duolink *in situ* PLA detection Kit (OLink; Bioscience, Uppsala, Sweden ref. DUO92008) following the instructions of the supplier. Primary neurons were grown on glass coverslips, fixed in paraformaldehyde (4%) for 15 min, washed with PBS containing glycine (20 mM) to quench the aldehyde groups and permeabilized with the same buffer containing Triton X-100 (0.05%, 20 min for primary neurons and 30 min for brain sections) and successively washed with PBS. Then, samples were incubated (1 h) at 37 °C with a blocking solution (ref. DUO82007, Sigma-Aldrich) in a pre-heated humidity chamber. After overnight incubation with the antibody diluent medium having a mixture of rabbit anti-GPR88 (1/100, ab64905, Abcam) and mouse anti-KOR (1/100, sc-374479, Santa Cruz Biotechnology Inc.) primary antibodies, ligation and amplification were conducted as indicated by the supplier. Samples were stored in Immu-mount® containing Hoechst 33432 (1/100) to stain nuclei. Samples were observed in a Zeiss 880 confocal microscope (Carl Zeiss, Oberkochen, Germany) equipped with an apochromatic 63 × oil immersion objective (N.A. 1.4) and 405 nm, 488 nm and 561 nm laser lines. For each field of view, two channels (one per staining) and four Z stacks with a step size of 1 μm were acquired. The number of D_1R^+ or D_2R^+ cells (green channel) containing one or more red dots versus total positive cells was determined, and a Student's t-test was used to compare the PLA signals (red dots/cell).

2.11. *siRNA transfection*

Primary striatal neurons were transiently transfected with the GPR88 siRNA (ref. sc-75192, Santa Cruz Biotechnology, Inc.) by the Lipofectamine 2000 method (ref. 11668-019, Invitrogen, Thermo Fisher Scientific, Waltham, MA, United States). A transfection mix containing 0.05 nmol of siRNA, 20 μL of Lipofectamine 2000, and 1 mL of Neurobasal® without serum (ref. 21103-049, Gibco®, Thermo Fisher Scientific, Waltham, MA, United States) final volume was incubated for 20 min at room temperature prior to being added on neurons. The transfected-neuron culture plate was incubated at 37 °C under 5% CO_2 for 48 h.

2.12. *MolBoolean experimental procedure*

The MolBoolean assay kit was obtained from Atlas Antibodies (Stockholm, Sweden) and the manufacturer's protocol was followed. Striatal neurons washed using PBS were fixed with ice-cold 4% formalin solution (1004969011; Merck -Sigma-Aldrich-) for 15 min. Samples were washed 3 times with PBS and permeabilized using TBS (ThermoFisher Scientific) 0.2% v/v Triton X-100 (142314.1611; Panreac) for 15 min. After washing for 2 min with TBS, samples were transferred to a humid chamber. The samples in glass microscope slides (SuperFrost®Plus; ref. 631–0108; VWR) were delimitated with a hydrophobic barrier created with of A-PAP Pen (Z672548; Merck). Blocking was done with Intercept Blocking Buffer (927–700001; LI-COR) for 1 h at 37 °C. The samples were incubated with a mouse monoclonal anti-KOR primary antibody (1/100, sc-374479, Santa Cruz) for 2 h at room temperature, followed by 3 min wash in TBS. Afterwards samples were incubated (overnight at 4 °C) with a rabbit polyclonal anti-GPR88 primary antibody (1/100, ab64905, Abcam). Primary antibodies were diluted in blocking buffer. The samples were then washed 3 times (3 min each) with 0.05% TBS-Tween20 (TBST; P5927; Merck -Sigma-Aldrich-) and incubated (for 1 h at 37 °C) with 3 μg/mL of each proximity probe (A and B), diluted in intercept blocking buffer.

Next, samples were washed once (3 min) in HBS-Tween20 (HSBT) and twice (3 min each) in TBST. Subsequently, cells were incubated (1 h at 37 °C) with 0.05 μM oligonucleotide sequence in T4 DNA ligase buffer supplemented with 0.25 mg/mL BSA (Merck-Sigma-Aldrich-), followed by a 3 min wash in HBST and a 3 min wash in TBST. Later, a mix of 0.125 U/μL Nt.*Bsm*AI (nickase enzyme) in NEBuffer CutSmart (New England Biolabs) and 0.25 mg/mL BSA was added (30 min at 37 °C). For the hybridization of the tag oligonucleotides, samples washed in TBST and then incubated (1 h at 37 °C) in TBS, 0.25 mg/mL BSA and 0.5 μM tag oligonucleotides A and B. Finally, ligation was achieved using 0.05 U/μL T4 ligase in T4 DNA ligase buffer containing 0.25 mg/mL BSA (1 h at 37 °C). Washed samples were incubated (90 min at 37 °C) in phi29 polymerase buffer (Monserate Biotechnology group; San Diego, CA), 0.25 mg/mL BSA, 1.25 mM dNTPs (Thermo Fisher Scientific), and 1 U/μL phi29 polymerase (Monserate Biotechnology group). Further washes with TBST preceded incubation (1 h at 37 °C) with detection mix (0.025 μM detection oligonucleotides A and B dissolved in TBS). Excess reagent was removed using HSB and later, TBS.

Slides were mounted with Shandon™ Immu-Mount™ (#9990402; ThermoFisher) and sealed with cover glass #1.5 (2980–244; Corning). Samples were observed in a Zeiss 880 confocal microscope (Carl Zeiss, Oberkochen, Germany) equipped with an apochromatic 63 × oil immersion objective (N.A. 1.4) and 405, 561 and 640 nm laser lines. For each field of view, three channels were considered (405 nm for nuclei in blue, 561 nm for KOR in red and 640 nm for GPR88 in green). Images from a minimum of 5 Z stacks with a step size of 0.5 μm were acquired.

2.13. *CellProfiler® data analysis*

Quantification and colocalization analyses of the rolling circle amplification products (RCPs) of PLA and MolBoolean assays were performed with specifically designed pipelines for the CellProfiler™ software on the deconvolved but otherwise unaltered images. Images were deconvolved with Parallel Spectral Deconvolution v1.12 plugin for ImageJ software applying the Tikhonov's algorithm, after calculating the appropriate Point Spread Function (PSF) by considering the refraction index of the Immu-mount®, numerical aperture of the objective and wavelength of the channel for deconvolution. Deconvolved split-channel images in grayscale format were analyzed using the CellProfiler™ software version 4.2.8:

For MolBoolean images analysis, a pipeline for RCPs quantification for ATTO565 (red dots, KOR) and ATTO647 (green dots, GPR88) that adjust the size for nuclei detection or the estimated area of each cell, was compiled with the following modules: *IdentifyPrimaryObjects, IdentifySecondaryObjects, EnhanceOrSuppressFeatures, GaussianFilter, IdentifyPrimaryObjects, ExpandOrShrinkObjects, IdentifySecondaryObjects, CombineObjects, MaskObjects, MeasureObjectIntensity, ClassifyObjects, FilterObjects, OverlayOutlines, SaveImages, RelateObjects,* and *ExportToSpreadsheet.*

For striatum section PLA image analysis, a pipeline for RCPs quantification (red dots) in the estimated areas of D_1R and D_2R positive cells was used. Pipeline was compiled with the following modules: *ColorTogray*, *Threshold*, *IdentifyPrimaryObjects, IdentifySecondaryObjects*, *MaskImage*, *EnhanceOrSuppressFeatures*, *ShrinkToObjectCenters*, *ExpandOrShrinkObjects*, *RelateObjects*, *SaveImages,* and *ExportToSpreadsheet*.

Corrections of brightness and contrast were made on Figure images to improve the visibility of RCPs.

To measure transfection efficiency, a CellProfiler® pipeline was designed to quantify transfected cells, defining cells as positive if they exceeded a specific fluorescence threshold. This pipeline included the

following CellProfiler® modules: *ColorToGray*, *IdentifyPrimaryObjects, IdentifySecondaryObjects*, *OverlayOutlines, SaveImages, RelateObjects,* and *ExportToSpreadsheet.*

2.14. Data handling and statistical analysis

GraphPad Prism 10 software (San Diego, CA, USA) was used for data analysis. One-way ANOVA followed by *post hoc* Dunnett's test were used when multiple comparison analysis were performed. BRET parameters were calculated using an *ad hoc* online tool (Herraez, 2022). In striatal neuron PLA images the number of red dots/cell was determined using Andy's algorithm Fiji's plug-in (Law et al., 2017). Two-tailed Student's t-test was used for PLA statistical analysis. Statistical analysis was undertaken only when each group size was at least n = 5, n being the number of independent variables (technical replicates were not treated as independent variables). Differences were considered significant when $P < 0.05$.

2.15. Ethical approval

Animal handling, sacrifice, and further experiments were conducted according to the guidelines set in Directive 2010/63/EU of the European Parliament and the Council of the European Union that are enforced in Spain by National and Regional organisms; the 3R rule (replace, refine, reduce) for animal experimentation was also considered. According to the current legislation, protocol approval is unnecessary if animals are

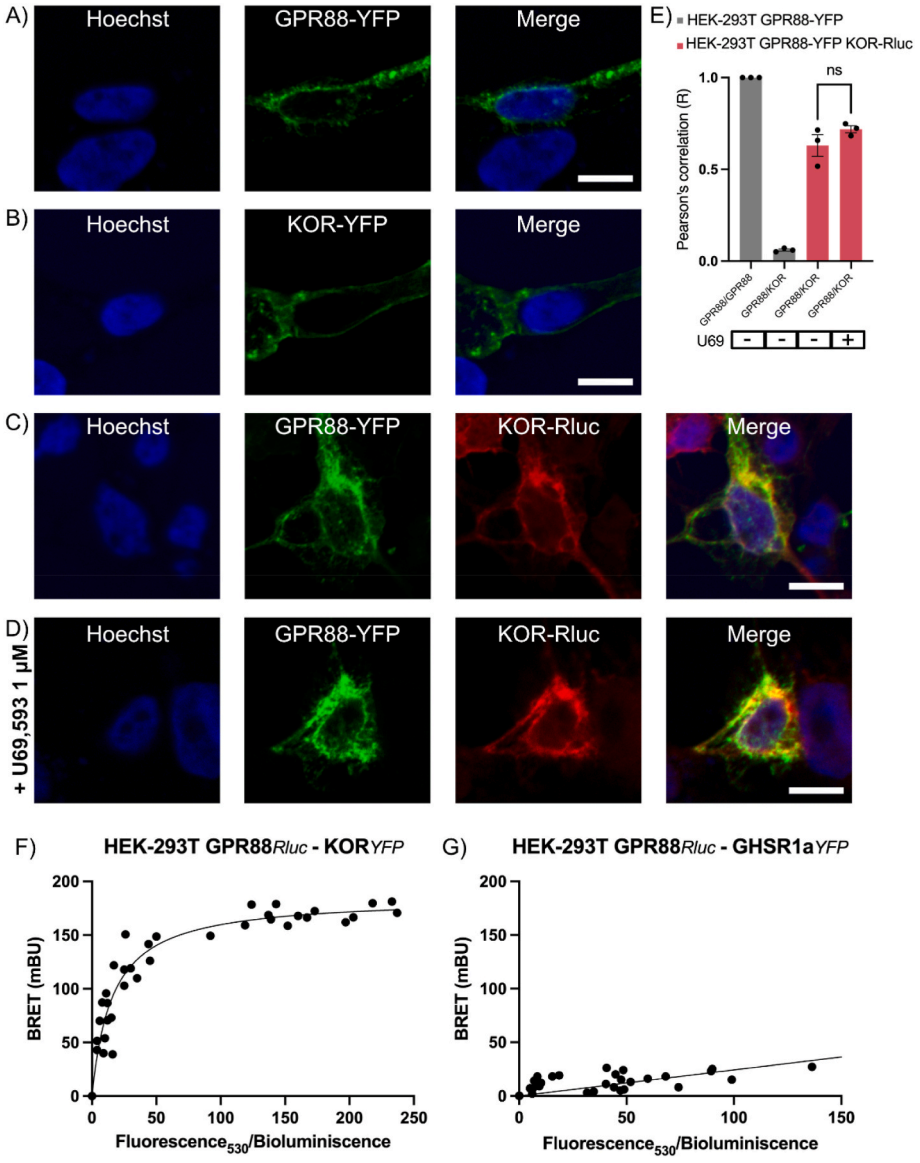

Fig. 1. Interaction between the human GPR88 and the human KOR in heterologous cells. Panels A–B. Images of HEK-293T cells expressing KOR-YFP (A) or GPR88-YFP (B), which were detected by fluorescence emission (green). Panels C–D. Immunocytochemistry performed in HEK-293T cells expressing GPR88-YFP, which was detected by fluorescence (green) and KOR-Rluc, which was detected by a mouse monoclonal anti-Rluc antibody and a secondary Cy3-conjugated anti-mouse IgG antibody (red). Colocalization is shown in yellow. Cell nuclei were stained with Hoechst 33432 (blue). Images were taken near the bottom of the cell, i.e. it mainly includes the membrane in contact with the glass of the plate. Scale bar: 10 µm. Panel E. Bar chart of GPR88-KOR colocalization, determined by calculating Pearson's coefficient (R). The statistical analysis was performed using a one-way ANOVA, followed by Dunnett's *post hoc* test for comparisons with the control group (GPR88/KOR untreated). $F(3,8) = 160.9$ $p < 0.001$. Panels F–G. BRET assays performed in HEK-293T cells transfected with a constant amount (0.5 µg) of cDNAs for GPR88-Rluc (donor), and increasing amounts of cDNA (0.25–2 µg) (F) for KOR-YFP (acceptor) or, as a negative control, using cDNA (0.25–1.5 µg) coding for GHSR1aR-YFP (G). Values are the mean ± S.E.M. of 6 independent experiments performed in duplicates. F: $BRET_{MAX} = 185.4 \pm 5.7$ mBU, $BRET_{50} = 16.0 \pm 2.1$ mBU. (For interpretation of the references to colour in this figure legend, the reader is referred to the web version of this article.)

sacrificed to obtain, as in the present study, a specific tissue.

3. Results

3.1. Interaction between GPR88 and KOR in HEK-293T cells

HEK-293T cells were transfected with cDNAs for GPR88 fused to yellow fluorescent protein (YFP) (Fig. 1A) or KOR-YFP (Fig. 1B); these receptors were observed at the plasma membrane level by detecting their expression by fluorescence. The degree of colocalization of GPR88 and KOR receptors was assessed in cotransfected cells using immunocytochemical techniques. Fig. 1C shows robust expression of the two receptors and a high degree of colocalization as assessed using Pearson's correlation coefficient. Pretreatment with the selective agonist for the KOR (U69,593) did not result in any significant change in the amount of colocalization of KOR-YFP and GPR88-Rluc (Fig. 1D) i.e. similar Pearson's correlation coefficient values were obtained in treated and untreated cells expressing both receptors (Fig. 1E). Bioluminescence resonance energy transfer (BRET) assays showed a hyperbolic relationship between the expression of the donor GPR88 fused to *Renilla* luciferase (Rluc) and the acceptor KOR-YFP that proves a direct interaction (within a 10 nm distance range). These results confirm those reported elsewhere using HEK-293T cells expressing Venus-tagged KOR and GPR88-Rluc (Fig. 1F). In contrast, GPR88 did not interact with another GPCR, the ghrelin receptor, as indicated by the linear relationship obtained using GPR88-Rluc and ghrelin receptor-YFP (Fig. 1G).

To ensure that the transfection protocol was optimized, expression controls for the KOR-YFP and GPR88-Rluc plasmids were performed. Transfection efficiency was quantified using a custom CellProfiler® pipeline that counted the total number of cells and identified as transfected those that exceeded a specific fluorescence threshold. The transfection efficiency was found to be 70.3% for the KOR-YFP plasmid and 71.9% for the GPR88-Rluc plasmid (Supplementary Fig. S1).

3.2. GPR88 expression and KOR-mediated signaling in HEK-293T cells

Preliminary experiments showed that GPR88 blunted the coupling of KORs to G_i in HEK-293T cells coexpressing the two receptors and treated with forskolin (FK) and U69,593, a selective KOR agonist. A concentration-response experiment measuring the effect of U69,593 on the FK-stimulated intracellular cAMP levels confirmed an inhibition exerted by the expression of GPR88. In HEK-293T cells expressing the KOR (grey) the IC_{50} value for the agonist was 3.1 nM, and cAMP levels were reduced by 21.4% compared to cAMP levels in only FK-stimulated cells. In cells coexpressing KOR and GPR88 receptors (red) the IC_{50} was similar (5.1 nM), while the reduction of cAMP levels was less pronounced (12.1%; Fig. 2A). We next investigated whether GPR88 altered other KOR-mediated signaling pathways. Phosphorylation of ERK1/2 is considered a measure of the degree of activation of the MAPK signaling pathway. U69,593 agonist concentration-response assays in cells expressing KOR (grey) or both receptors (red) showed that expression of GPR88 abolished the link of KOR to MAPK pathway activation (Fig. 2B).

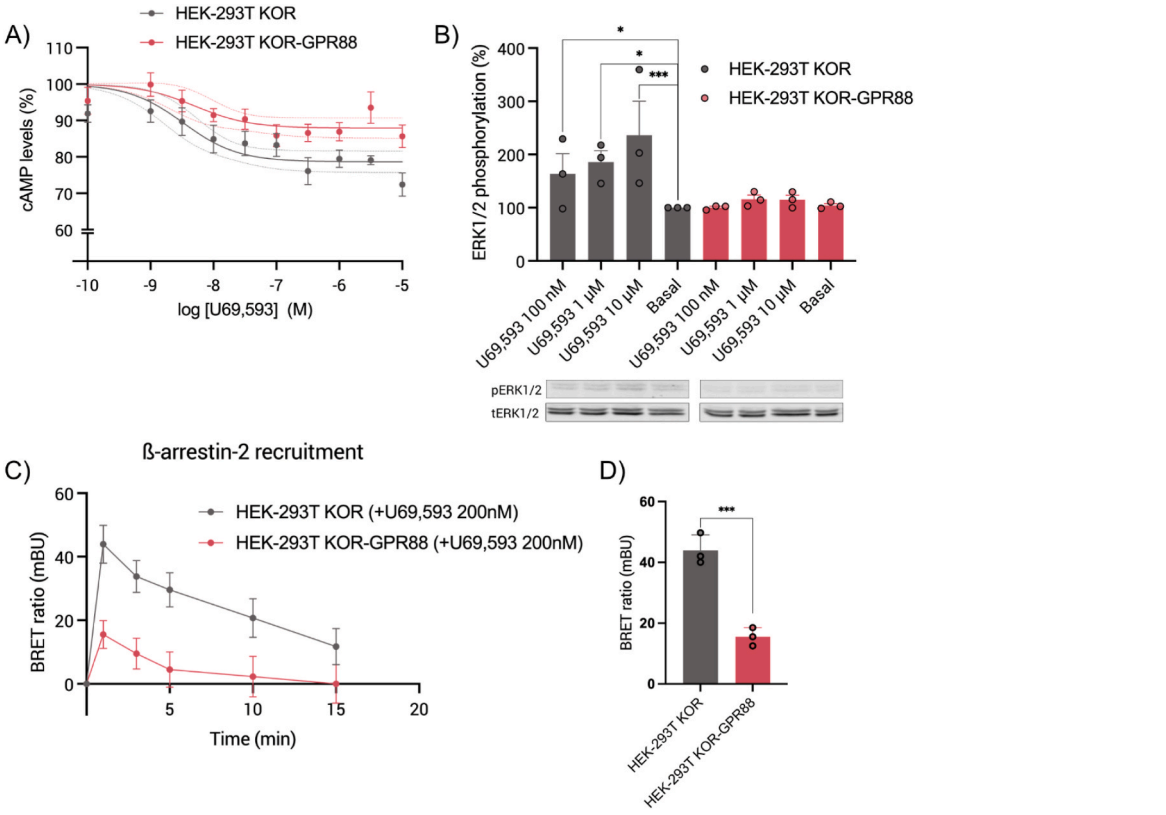

Fig. 2. Signaling via the KOR in the absence and presence of GPR88. HEK-293T cells transfected with the cDNAs (1 µg) for KOR (grey) or with the cDNAs for KOR and GPR88 (1 µg each) (red) were treated with 0.5 µM forskolin (FK, 15 min) and, subsequently, with different concentrations of U69,593, a selective agonist of KOR. Panel A. Intracellular cAMP levels were determined by TR-FRET as described in Methods. Values are the mean ± S.E.M. of data from 6 independent experiments performed in triplicates. Panel B. ERK1/2 phosphorylation assessed by western blotting. Results are expressed as a percentage versus basal condition. In ERK1/2 phosphorylation assays, the statistical analysis was performed using a one-way ANOVA, followed by Dunnett's *post hoc* test for comparisons with the control group (basal; *$p < 0.05$, **$p < 0.01$, ***$p < 0.001$). $F(7, 16) = 3.288$. $p = 0.0231$. Panel C. ß-arrestin-2 recruitment time response assays were performed in HEK-293T cells expressing KOR-YFP, ß-arrestin-2-Rluc and, when indicated, GRP88. Time was counted upon addition of 200 nM U69,593. Panel D. Bar graphs represent the mean ± S.E.M. of the maximum BRET derived from ß-arrestin-2 recruitment in the absence (grey) or presence of GPR88 (red) ***Unpaired *t*-test two tailed, $t(4) = 8.287$. $p = 0.0012$. (For interpretation of the references to colour in this figure legend, the reader is referred to the web version of this article.)

Finally, and in alignment with the other signaling pathways studied, β-arrestin 2-recruitment cellular assays showed that GPR88 expression significantly decreased the signal achieved by the KOR agonist (Fig. 2C). In cells transfected with cDNA for KOR (grey) the $BRET_{MAX}$ for β-arrestin-2 recruitment was 43.9 mBU, whereas in cells coexpressing GPR88 and KOR (red) the $BRET_{MAX}$ was reduced to 15.5 mBU (Fig. 2D). In summary activation of the KOR in the presence of GPR88 leads to poor responses in terms of reduction of cAMP levels and to a failure to signal towards the MAPK signaling pathway or to recruit β-arrestin-2.

3.3. GPR88 deletion restores the effect of a selective KOR agonist in striatal primary neurons

To assess the physiological relevance of the findings in the heterologous system and due to the marked expression of GPR88 in the striatum, experiments were conducted in mice striatal neurons. For PLA primary antibodies that are specific for GPR88 and for KOR were used. PLA allows demonstrating protein-protein interactions in natural sources. The negative control was obtained omitting the anti-KOR antibody (Fig. 3A). Data in Fig. 3B show that complexes formed by GPR88 and

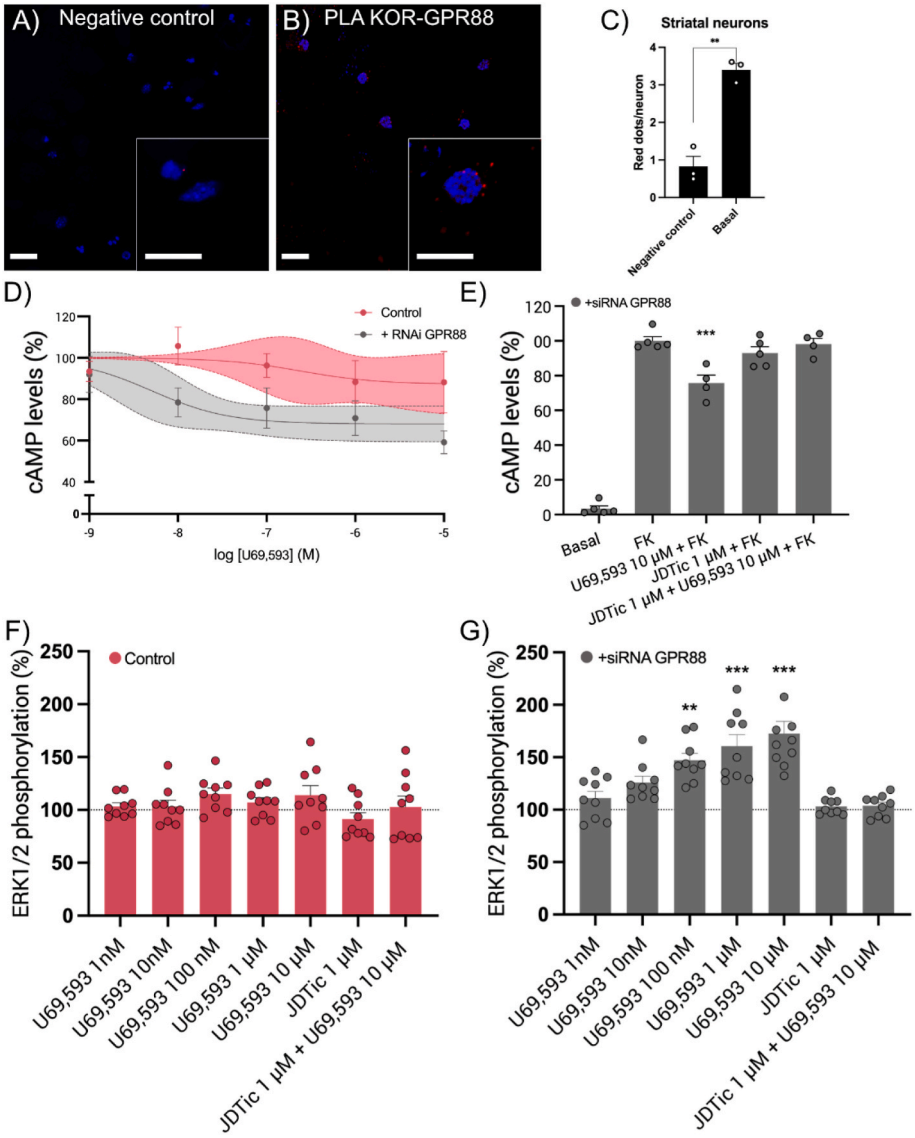

Fig. 3. Interaction between GPR88 and KOR and KOR-mediated signaling in primary striatal neurons. Panels A–C. Expression of KOR-GPR88 heteromers in mouse striatal neurons determined by PLA. As a negative control of the assay, incubation with one of the secondary antibodies was omitted. Confocal microscopy images (stacks of 3 consecutive panels) show heteroreceptor complexes as red clusters, and Hoechst 33432-stained nuclei (blue). Three independent experiments were performed for each condition. Scale bar: 10 μm. Bar graph (C) shows the amount of red clusters/cell (Unpaired *t*-test two tailed $t(4) = 8.077$; $^{**}p = 0.0013$). Panel D. Cells in which cAMP production was induced by 0.5 μM forskolin (FK) were treated with the selective agonist for KOR (10 μM U69,593) and/or the selective antagonist for KOR (1 μM JDTic) and cAMP levels were determined. Experiments were performed in untransfected neurons and in neurons transfected with a siRNA that suppresses the expression of the GPR88 gene. The statistical analysis was performed using a one-way ANOVA, followed by Dunnett's post hoc test: $^{***}p < 0.001$ versus FK treatment; $F(4,18) = 177.7$. Panel E. Reduction of FK-induced increases in cAMP levels were measured using different concentrations of U69,593 in neurons untreated (red) or transfected with a siRNA that suppresses GPR88 gene expression (grey). Data points and 95% confidence intervals (CI) are shown. ERK1/2 phosphorylation was assessed using AlphaScreen®SureFire® kit (PerkinElmer). Results are expressed as a percentage versus basal (dotted line). Panel F. ERK1/2 phosphorylation assay was performed in primary neurons. Panel G. ERK1/2 phosphorylation assay was performed in primary neurons transfected with a siRNA that suppresses GPR88 gene expression. In MAPK pathway activation assays, the statistical analysis was performed using a one-way ANOVA, followed by Dunnett's *post hoc* test for comparisons with basal) ($^{**}p < 0.01$, $^{***}p < 0.001$ versus vehicle treatment). Panel F, $F(7, 61) = 1.288$. $p = 0.2724$. Panel G, $F(7, 61) = 13.83$. $p < 0.001$. (For interpretation of the references to colour in this figure legend, the reader is referred to the web version of this article.)

KOR are present in some striatal neurons (detected as red dots). The number of red dots per neuron displaying at least one red dot was approximately 4, suggesting a significant expression of GPR88/KOR heteromers (Fig. 3C). Based on the results outlined above, a relatively high proportion of heteromers would correlate with reduced KOR-mediated signaling. To test this hypothesis, the effect of U69,593 on FK-induced intracellular cAMP levels was measured in concentration-response experiments in primary striatal neurons (red). The modest effect of the agonist was markedly enhanced when GPR88 siRNA (grey) was transfected to downregulate GPR88 expression (Fig. 3D). The U69,593 effect was specific because it was completely blocked by pre-treatment with the selective KOR antagonist, JDTic (1 μM) (Fig. 3E).

To determine whether KOR signal blockade, mediated by KOR-GPR88 heteromer expression, also affects signaling through the MAPK pathway in striatal neurons, assays were conducted to measure ERK1/2 phosphorylation. A concentration-response experiment with U69,593 (1 nM–10 μM) revealed no significant phosphorylation of ERK1/2 (Fig. 3F), consistent with results from HEK-293T cells coexpressing both GPR88 and KOR receptors (Fig. 2B). In contrast, striatal neurons in which GPR88 expression was silenced via siRNA transfection showed restored KOR signaling through the MAPK pathway (Fig. 3G). Additionally, this increment on ERK1/2 phosphorylation, mediated by KOR activation with U69,593, was abolished by pretreatment with JDTic (Fig. 3G). These results demonstrate in mice primary neurons that GPR88 is naturally expressed and significantly inhibits the G_i-coupling of the KOR and KOR-mediated ERK1/2 phosphorylation.

3.4. Quantification of KOR-GPR88 heteromerization in primary striatal neurons and KOR-GPR88 complexes localization in the direct and indirect pathways of the basal ganglia

The MolBoolean technique is unique in assessing the amount of receptors that are interacting versus those that are not forming heteromers. We applied the MolBoolean assay to primary striatal neurons to determine the extent of interaction between KOR and GPR88 receptors. Deconvolution of acquired images facilitated subsequent processing and quantification of free receptors (KOR monomers visualized as red dots in Fig. 4A; GPR88 monomers as green dots in Fig. 4B) and KOR-GPR88 heteromers (visualized as yellow dots in the merged ATTO565 and ATTO647 channels, Fig. 4D). Nuclei were stained with Hoechst 33432 and are shown in blue (Fig. 4C). Quantification using a custom CellProfiler® pipeline (see Methods) revealed that the majority of KOR and GPR88 receptors in each neuron formed heteromers, representing approximately 79% of the total RCPs detected (Fig. 4E). Thus, free KOR and GPR88 receptors represent minor populations, comprising, respectively, 6.6% and 14.4% of the total RCPs detected (Fig. 4E). Control experiments omitting either the anti-KOR (Supplementary Fig. 2 panels A–B) or anti-GPR88 (Supplementary Fig. 2 panels C–D) primary antibody resulted in only a single signal without overlap. Similarly, omitting either of the two specific oligonucleotide probes (probe A, Supplementary Fig. 2 panels E–F; probe B, panels G–H) yielded a single signal. These controls confirm the MolBoolean assay's specificity.

A further objective was to determine whether heteromer expression was consistent across medium spiny neurons (MSNs) in both the direct and indirect pathways, characterized respectively by neurons expressing dopamine D_1 and D_2 receptors. PLA was used to detect GPR88-KOR heteromers were combined with immunodetection of dopamine D_1 and D_2 receptors using Alexa Fluor-conjugated primary antibodies. Experiments conducted on mouse striatal sections revealed that a higher percentage of D_1R^+ cells expressed the heteromer (75.8% of total D_1R^+ cells, Fig. 5B–C) (at least one red dot) compared to D_2R^+ cells (42.3% of total D_2R^+ cells, Fig. 5E–F). This finding indicates that the heteromer is more prevalent in the direct pathway than in the striatopallidal indirect pathway. As a negative control, omitting one secondary antibody resulted in negligible signal (Fig. 5 Panels A, D).

4. Discussion

Deorphanization of GPR88 is essential for understanding its physiological roles, as this receptor is highly expressed in brain regions involved in reward and motor control. Identifying its endogenous ligand is crucial, as without this knowledge, GPR88 cannot be fully evaluated as a therapeutic target for CNS diseases. Meanwhile, studies on this orphan receptor continue to yield valuable insights.

In Parkinson's disease models, such as the hemilesioned rat, GPR88 expression is elevated in striatonigral and reduced in striatopallidal MSNs (Meirsman et al., 2016). This altered expression in parkinsonism highlights the receptor's potential involvement in motor disorder pathology. However, the discovery of heteromers with KOR and the GPR88-mediated regulation of KOR activation by opioids suggest that the role of this orphan receptor extends beyond motor control.

GPR88 is expressed in enkephalinergic and substance P projection MSNs of the striatum, i.e. it is coexpressed with dopamine receptors in both direct and indirect striatal pathways (Massart et al., 2009). Our findings add further insight, revealing a higher proportion of D_1 receptor-expressing neurons that contain GPR88/KOR heteromers (75.8% in D_1R^+ cells versus 42.4% in D_2R^+ cells, Fig. 5). Beyond motor control, the direct pathway facilitates the initiation and execution of reward-oriented behaviors, while the indirect pathway inhibits impulsive or inappropriate behaviors. The differential expression observed suggests that GPR88-KOR heteromers may play a greater role in reward processing than in pain perception.

The results presented here, alongside previous findings (Laboute et al., 2020), suggest that GPR88 interacts with opioid receptors, and regulates the effect of opioids at the CNS. This antagonism was reported to be less pronounced for KORs compared to delta (δ) and mu (μ) opioid

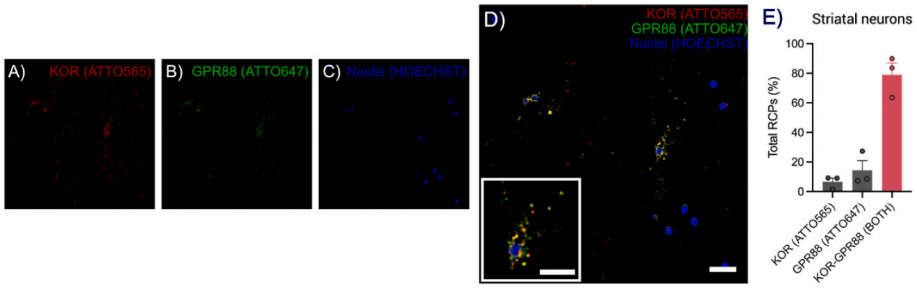

Fig. 4. MolBoolean analysis of GPR88 and KOR expression in striatal neurons. Label for KOR is in red (Panel A), label for GPR88 is in green (Panel B), and label for KOR-GPR88 complexes is in yellow (Panel D). Hoechst 33432 staining of nuclei is shown in blue (Panel C). Scale bar = 15 μm. Panel E. Quantification of RCPs is expressed as a percentage of the total RCPs (the sum of red, green, and yellow dots) obtained in each field of view. Values in the bar graphs are the mean ± S.E.M. from data of three independent experiments performed in duplicates. (For interpretation of the references to colour in this figure legend, the reader is referred to the web version of this article.)

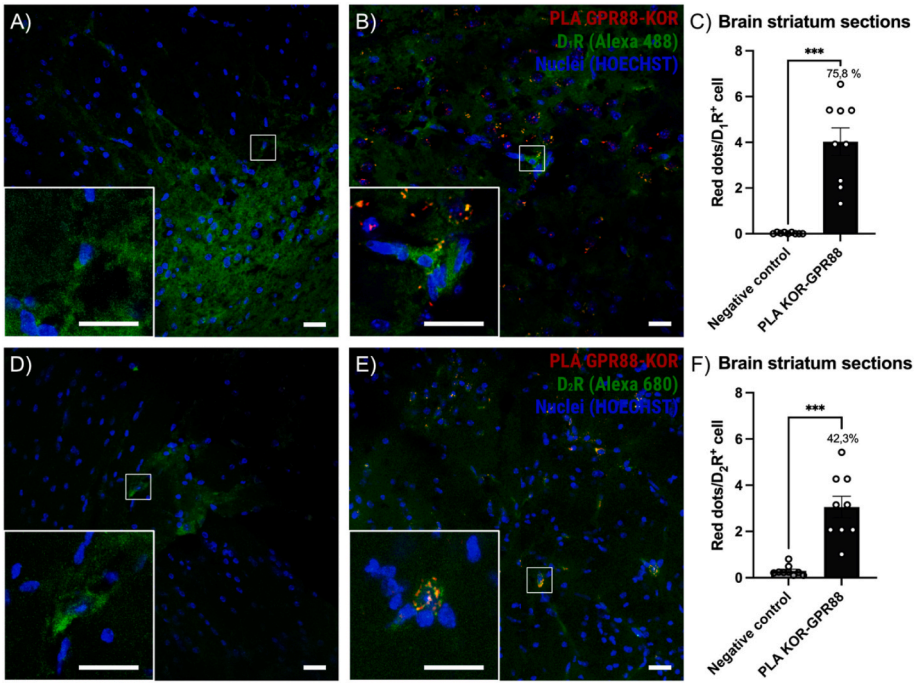

Fig. 5. Distribution of GPR88-KOR heteromers in cells expressing D_1 or D_2 receptors in mouse striatal sections. Expression of KOR-GPR88 heteromers in mouse striatal sections was determined by PLA. As a negative control of the assay, incubation with one of the secondary antibodies was omitted (Panel A, D). Confocal microscopy images (stacks of 3 consecutive panels) show GPR88-KOR heteroreceptor complexes as red clusters near D_1R (Panel B) or D_2R (Panel E) positive cells (Alexa 488 or Alexa 680). Nuclei were Hoechst 33432-stained (blue). Panel C. Bar graph shows the amount of red clusters/cell in D_1R^+ cells (*** Unpaired *t*-test two tailed $t(16) = 6.628$; $p < 0.001$ versus the negative control condition). Panel F. Bar graph shows the amount of red clusters/cell in D_2R^+ cells (*** Unpaired *t*-test two tailed $t(16) = 5.841$; $p < 0.001$ versus the negative control condition). Three independent experiments were performed for each condition. Scale bar: 10 μm. Numbers above the right bar in panels C and F represent the percentage of neurons expressing GPR88-KOR heteromers. (For interpretation of the references to colour in this figure legend, the reader is referred to the web version of this article.)

receptors. Specifically, the impact of GPR88 expression on the effect of the KOR agonist, U50488H, was modest, 27.7% reduction of the maximal effect on cAMP levels, contrasting with the 61.1% observed with the δ receptor agonist (Laboute et al., 2020). The qualitative differences on comparing to the results here reported could stem from the use of distinct agonists. In the current study, the KOR-selective agonist U69,593 exhibited high potency across various signaling assays, including reduction of FK-induced cAMP production, β-arrestin-2 recruitment and ERK1/2 phosphorylation. The coexpression of GPR88 significantly attenuated all responses elicited by U69,593 on KORs. Moreover, the antagonistic role of GPR88 was further corroborated in primary neurons treated with small interfering RNA that suppressed GPR88 expression. While the physiological implications of GPR88-mediated antagonism of opioid receptors remain elusive, inhibiting these receptors may be crucial in modulating drug addiction and other CNS pathologies. Notably, a small proportion of GPR88 and KOR receptors were found not to form heteromers (Fig. 4). For comparison, we observed qualitatively different results with the heavily-studied heteromer composed of adenosine A_{2A} and dopamine D_2 receptors (Hillion et al., 2002). Using the Molboolean technique in striatal samples from rodents and non-human primates we found that many of the D_2 receptor molecules are forming heteromers, whereas the A_{2A} receptor is less engaged in heteromeric interactions with the dopamine D_2 receptors (Rivas-Santisteban et al., 2023).

Opioids, via the KOR-mediated dopamine release, play a significant role in mood regulation, reward, and motivation. By modulating KOR activity, GPR88 may influence dopamine pathways in a way that could be beneficial for treating disorders characterized by dopamine dysregulation, such as schizophrenia or bipolar disorder. Inhibiting the KOR can offer multiple therapeutic benefits, particularly for neuropsychiatric disorders and pain management (Alam and Singh, 2023; Aldrich and McLaughlin, 2009; Lambert, 2023). This approach could alleviate depression and anxiety by counteracting the dysphoric and anxiogenic effects associated with kappa receptor activation. It also has the potential to mitigate the adverse impacts of stress, thereby lowering the risk of stress-related psychiatric conditions. KOR inhibition could play a significant role in treating addiction and preventing relapse by reducing the rewarding effects of drugs like cocaine and alcohol. Finally, KOR inhibition may benefit conditions linked to dopamine dysregulation, such as Parkinson's disease.

The difficulty in identifying endogenous ligands for some orphan receptors shifts the focus to other properties of GPCRs. For GPR88, the discovery of several interacting receptors underlines the importance of a receptor with such highly regulated expression in several neuronal types of the striatum (Massart et al., 2009). In addition to opioid receptors, GPR88 can interact with at least three other GPCRs relevant for dopaminergic transmission, namely dopamine D_2, adenosine A_{2A} and orexin OX_1 receptors (Laboute et al., 2020; Chen et al., 2015). It turns out that the kappa opioid receptor-orexin 1 receptor heteromer leads to increased phosphorylation of CREB, a cAMP-response element-binding protein (Chen et al., 2015). pCREB targets the nucleus where it activates the transcription of, among others, Ppp1r1b, which encodes DARPP-32, a protein that regulates dopamine signaling (Babenko et al., 2020; Girault and Nairn, 2021). In summary, the potential interactions of GPR88 with KOR, dopamine D_2, adenosine A_{2A}, and orexin OX_1 receptors in the different neuronal types present in striatum open new perspectives for understanding its role in motor control and reward circuits. This emphasizes the importance of mapping the expression of GPR88-containing heteromers and further exploring GPR88's functions and its contributions to dopaminergic transmission.

CRediT authorship contribution statement

Rafael Rivas-Santisteban: Writing – review & editing, Writing –

original draft, Validation, Investigation, Formal analysis, Conceptualization. **Jaume Lillo:** Writing – review & editing, Methodology, Investigation. **Claudia Garrigós:** Writing – review & editing, Investigation. **Gemma Navarro:** Writing – review & editing, Supervision, Resources, Methodology, Investigation, Conceptualization. **Rafael Franco:** Writing – review & editing, Writing – original draft, Supervision, Resources, Data curation, Conceptualization.

Funding

This work was supported by grants PID2020-113430RB-I00 and PID2021-126600OB-I00 funded by Spanish MCIN/AEI/10.13039/501100011033 and, as appropriate, by "ERDF A way of making Europe", by the "European Union" or by the "European Union Next Generation EU/PRTR". The research group of the University of Barcelona is considered of excellence (grup consolidat #2021 SGR 00304) by the Regional Catalonian Government. CG received from the Spanish Ministry of Science and Innovation (MCIN) and Spanish Investigation Agency (AEI: Agencia Estatal de Investigación) a FPI predoctoral contract, PRE2022-104618 ("Formación de Personal Investigador"; contratos predoctorales para la formación de doctores"). This contract is associated with the PID2021-126600OB-I00 grant.

Declaration of competing interest

The authors declare that they have no known competing financial interests or personal relationships that could have appeared to influence the work reported in this paper.

Appendix A. Supplementary data

Supplementary data to this article can be found online at https://doi.org/10.1016/j.neuropharm.2024.110242.

Data availability

Data will be made available on request.

References

Alam, M.R., Singh, S., 2023. Neuromodulation in Parkinson's disease targeting opioid and cannabinoid receptors, understanding the role of NLRP3 pathway: a novel therapeutic approach. Inflammopharmacology 31, 1605–1627.
Aldrich, J.V., McLaughlin, J.P., 2009. Peptide kappa opioid receptor ligands: potential for drug development. AAPS J. 11, 312–322.
Alexander, S.P.H., et al., 2023. The Concise Guide to PHARMACOLOGY 2023/24: G protein-coupled receptors. Br. J. Pharmacol. 180 (Suppl. 2), S23–S144.
Alkufri, F., Shaag, A., Abu-Libdeh, B., Elpeleg, O., 2016. Deleterious mutation in GPR88 is associated with chorea, speech delay, and learning disabilities. Neurol. Genet. 2.
Babenko, V.N., Galyamina, A.G., Rogozin, I.B., Smagin, D.A., Kudryavtseva, N.N., 2020. Dopamine response gene pathways in dorsal striatum MSNs from a gene expression viewpoint: CAMP-mediated gene networks. BMC Neurosci. 21, 1–14.
Brooks, J.M., O'Donnell, P., 2017. Kappa opioid receptors mediate heterosynaptic suppression of hippocampal inputs in the rat ventral striatum. J. Neurosci. 37, 7140–7148.
Chen, J., et al., 2015. Heterodimerization of human orexin receptor 1 and kappa opioid receptor promotes protein kinase A/cAMP-response element binding protein signaling via a Gαs-mediated mechanism. Cell. Signal. 27, 1426–1438.
Escobar, A.P., 2017. The role of kappa opioid receptors in glutamate input selection in the ventral striatum. J. Neurosci. 37, 11072–11073.
Franco, R., et al., 2018. N-Methyl-D-Aspartate receptor link to the MAP kinase pathway in cortical and hippocampal neurons and microglia is dependent on calcium sensors and is blocked by α-synuclein, tau, and phospho-tau in non-transgenic and transgenic APPSw,Ind mice. Front. Mol. Neurosci. 11, 273.
Girault, J.A., Nairn, A.C., 2021. DARPP-32 40 years later. Adv. Pharmacol. 90, 67–87.
Herraez, A., 2022. BRET analysis. https://biomodel.uah.es/lab/calculos/regresion/BRET.htm.
Hillion, J., et al., 2002. Coaggregation, cointernalization, and codesensitization of adenosine A2A receptors and dopamine D2 receptors. J. Biol. Chem. 277, 18091–18097.
Hradsky, J., Mikhaylova, M., Karpova, A., Kreutz, M.R., Zuschratter, W., 2013. Super-resolution microscopy of the neuronal calcium-binding proteins Calneuron-1 and Caldendrin. Methods Mol. Biol. 963, 147–169.
Laboute, T., et al., 2020. The orphan receptor GPR88 blunts the signaling of opioid receptors and multiple striatal GPCRs. Elife 9.
Lambert, D.G., 2023. Opioids and opioid receptors; understanding pharmacological mechanisms as a key to therapeutic advances and mitigation of the misuse crisis. BJA open 6, 100141.
Law, A.M.K., et al., 2017. Andy's Algorithms: new automated digital image analysis pipelines for Fiji. Sci. Rep. 7, 15717.
Logue, S.F., et al., 2009. The orphan GPCR, GPR88, modulates function of the striatal dopamine system: a possible therapeutic target for psychiatric disorders? Mol. Cell. Neurosci. 42, 438–447.
Massart, R., Guilloux, J.P., Mignon, V., Sokoloff, P., Diaz, J., 2009. Striatal GPR88 expression is confined to the whole projection neuron population and is regulated by dopaminergic and glutamatergic afferents. Eur. J. Neurosci. 30, 397–414.
Meirsman, A.C., et al., 2016. Mice lacking GPR88 show motor deficit, improved spatial learning, and low anxiety reversed by delta opioid antagonist. Biol. Psychiatr. 79, 917–927.
Mizushima, K., et al., 2000. A novel G-protein-coupled receptor gene expressed in striatum. Genomics 69, 314–321.
Quintana, A., et al., 2012. Lack of GPR88 enhances medium spiny neuron activity and alters motor- and cue-dependent behaviors. Nat. Neurosci. 15, 1547–1555.
Rivas-Santisteban, R., et al., 2023. Boolean analysis shows a high proportion of dopamine D2 receptors interacting with adenosine A2A receptors in striatal medium spiny neurons of mouse and non-human primate models of Parkinson's disease. Neurobiol. Dis. 188.
Trifilieff, P., Martinez, D., 2013. Kappa-opioid receptor signaling in the striatum as a potential modulator of dopamine transmission in cocaine dependence. Front. Psychiatr. 4, 50513.
Waes, V. Van, Tseng, K.Y., Steiner, H., 2011. GPR88: a putative signaling molecule predominantly expressed in the striatum: cellular localization and developmental regulation. Basal Ganglia 1, 83–89.
Wang, S., 2019. Historical review: opiate addiction and opioid receptors. Cell Transplant. 28, 233–238.